

Analytic Approach to the Stability of Standing Accretion Shocks: Application to Core-Collapse Supernovae

J. Martin Laming¹

ABSTRACT

We explore an analytic model of the accretion shock in the post bounce phase of a core-collapse supernova explosion. We find growing oscillations of the shock in the $l = 1$ and $l = 2$ modes, in agreement with a variety of existing numerical simulations. For modest values of the ratio of the outer accretion shock to that of the inner boundary to the shocked flow, the instability appears to derive from the growth of trapped sound waves, whereas at higher values, postshock advection clearly plays a role. Thus the model described here may relate to the different mechanisms of instability recently advocated by Blondin & Mezzacappa, and by Foglizzo and collaborators.

Subject headings: supernovae: general—hydrodynamics—instabilities—shock waves

1. Introduction

There is a growing consensus that a large fraction of core-collapse supernovae, possibly including the whole subset of Type Ib/c events, undergo significantly asymmetrical explosions. While clearly rotation and magnetic fields may play some role in this, instability associated with the stalled shock that forms at a radius of 100-300 km and lasts for a few hundred microseconds post bounce offers the intriguing possibility of generating asymmetrical explosions from a symmetrical progenitor, since such instability is usually dominated by low mode $l = 1, 2$ oscillations of the shock front. The original speculation for the origin of such

¹E. O Hulburt Center for Space Research, Naval Research Laboratory, Code 7674L, Washington DC 20375

oscillations (Herant et al. 1992; Herant 1995) in terms of convection behind the shock, following Chandrasekhar (1961) has been revised in recent years. Foglizzo, Scheck & Janka (2006) demonstrate that post shock advection can stabilize convective instability (Chandrasekhar (1961) only deals with a static case), and that convection alone cannot produce the dominant $l = 1, 2$ modes. In adiabatic simulations of gas with polytropic index $4/3$, which as shown by Janka (2001) is a good description of shocked inner regions of a core-collapse supernova, Blondin, Mezzacappa & DeMarino (2003) were the first to associate the instability with the shock itself. Blondin & Mezzacappa (2006) attributed this to the growth of trapped sound waves, travelling essentially laterally around the central accretor. This must be a purely shock driven instability, since convection is absent, and hence qualitatively different to the original speculations (Herant et al. 1992; Herant 1995). On the other hand, Foglizzo et al. (2007) and Galletti & Foglizzo (2005) attribute this shock-driven instability to an “advective-acoustic” cycle, originally introduced by Foglizzo (2002) in the context of black hole accretion flows. Vorticity perturbations generated at the distorted shock front advect inwards, and couple with outgoing sound waves at the inner boundary of the post-shock accretion flow. Upon reaching the outer shock, these sound waves further distort the shock front, leading to a positive feedback. While the mechanisms of Blondin & Mezzacappa (2006) and Foglizzo (2002) appear to produce similar outcomes in non-rotating cases, indeed Foglizzo et al. (2007) actually confirm the numerical values of frequencies and growth rates measured by Blondin & Mezzacappa (2006), it is possible the presence of rotation might lead to substantial differences, which we discuss further below.

Instabilities of the accretion shock also are observed in simulations with a more accurate treatment of supernova microphysics, with a realistic equation of state, neutrino transport and attendant nuclear reactions, and more physically motivated boundary conditions. Scheck et al. (2004) and Scheck et al. (2006) investigate the role of such instabilities in generating pulsar natal kicks, while Kifonidis et al. (2005) study the ejection of metal clumps to the outer regions of supernova ejecta. Burrows et al. (2006) also see the standing accretion shock instability 100 - 300 ms postbounce. The important feature of their simulation, though, is a core gravity wave at late times that transfers acoustic power to the shock to continue powering the explosion, the initial perturbation for which is possibly seeded by the accretion shock instability. Burrows et al. (2006) also favor the interpretation of Foglizzo et al. (2007) of an advective-acoustic cycle, though in this and the other more realistic simulations cited above, the exact mechanism of instability is difficult to identify. To avoid this problem, Ohnishi, Kotake & Yamada (2006) performed numerical simulations based on unperturbed spherically symmetrical shock accretion flows given by Yamasaki & Yamada (2005), a sort of “middle ground” between the adiabatic flows of Blondin, Mezzacappa & DeMarino (2003) and Blondin & Mezzacappa (2006) and the full

supernova simulations of other workers. Ohnishi, Kotake & Yamada (2006) clearly identify and measure growth rates for $l = 1$ and 2 mode instabilities. The real parts of the frequencies scale with $\int_{r_i}^{r_s} (1/c_s + 1/v_r) dr$, the integral between the inner radius of the accretion flow and the shock of the sum of the inverses of the sound speed and advection speed, suggesting that an advective-acoustic mechanism, as advanced by Foglizzo (2002) and Foglizzo et al. (2007), is at work. However Ohnishi, Kotake & Yamada (2006) only perturb the radial velocity component of the initially spherical symmetrical unperturbed flow, which may unduly influence their results, compared to allowing perturbations in polar and azimuthal directions as well. Yamasaki & Yamada (2006) include rather more physics, and again based on the frequencies at which modes grow, conclude that an advective-acoustic cycle is at work.

In this work we present another approach to the problem. Following the work of Vishniac & Ryu (1989) on planar shocks in the interstellar medium, we derive an approximate dispersion relation for oscillations of the accretion shock by adding the effect of a gravitational field and spherical geometry. In the case that the postshock advection is neglected, a quartic equation (actually a quadratic in ω^2 where ω is the frequency of oscillation) results, becoming a quintic equation in ω with the inclusion of advection. We find that in both cases for $\gamma \sim 4/3$, for all except the highest values of the ratio of the shock radius to the radius of the inner boundary, modes with $l = 1$ grow the fastest (in fact for cases where the postshock radial velocity, $u_r = 0$, no other nonradial modes grow). This suggests that for $l = 1$ in $\gamma = 4/3$ gas in this regime, postshock advection is not crucial to the operation of the instability. Thus in general these results will support the conclusions of Blondin & Mezzacappa (2006) that the instability proceeds by the growth of trapped waves in this regime. Nevertheless, regions of l and γ parameter space exist where we find modes that are only unstable in the presence of postshock advection, which we interpret as an advective-acoustic cycle, as suggested by Galletti & Foglizzo (2005) and Foglizzo et al. (2007). In both cases, the frequencies of the growing modes are similar, suggesting that frequency alone is not a good discriminator of the mechanism of instability. As will be seen below, this might be expected in a comparison of a perturbation advected radially between the shock and inner boundary, and a sound wave traveling essentially laterally around the shock.

2. Analytic Theory

We consider an unperturbed model in which spherically accreting plasma is decelerated at a spherically symmetrical shock, before accreting onto a protoneutron star. The accretion shock is at radius r_s , and we take an inner boundary at r_i , maintained at constant

pressure, where plasma cools and decouples from the postshock flow. The postshock flow is modeled by the Bernoulli equation, as given in Appendix A. Gas with polytropic index $\gamma < 1.5$ decelerates, and gas with $\gamma > 1.5$ accelerates away from the shock towards the inner boundary. We shall be solely concerned with $\gamma < 1.5$. The dominant variations with radius are in pressure and density, as shown in Figure 1.

To treat the perturbation, we follow in large part the methods and notation of Vishniac & Ryu (1989) who derive an approximate dispersion relation for application to shocks with arbitrary postshock structure. In spherical coordinates, we write the hydrodynamic equations; an equation of continuity and momentum equations in the r , θ and ϕ directions as

Continuity:

$$\begin{aligned} & \frac{\partial(\rho + \Delta\rho)}{\partial t} + (u_r + v_r) \frac{\partial(\rho + \Delta\rho)}{\partial r} + \frac{v_\theta}{r} \frac{\partial(\rho + \Delta\rho)}{\partial \theta} + \frac{(u_\phi + v_\phi)}{r \sin \theta} \frac{\partial(\rho + \Delta\rho)}{\partial \phi} \\ & + (\rho + \Delta\rho) \left[\frac{1}{r \sin \theta} \frac{\partial \sin \theta v_\theta}{\partial \theta} + \frac{1}{r \sin \theta} \frac{\partial (u_\phi + v_\phi)}{\partial \phi} + \frac{1}{r^2} \frac{\partial (r^2 (u_r + v_r))}{\partial r} \right] = 0 \end{aligned} \quad (1)$$

Radial Force:

$$\begin{aligned} (\rho + \Delta\rho) \left[\frac{\partial(u_r + v_r)}{\partial t} + (u_r + v_r) \frac{\partial(u_r + v_r)}{\partial r} + \left(\frac{u_\phi + v_\phi}{r \sin \theta} \right) \frac{\partial(u_r + v_r)}{\partial \phi} - \frac{(u_\phi + v_\phi)^2}{r} \right] \\ = - \frac{\partial(P + \Delta P)}{\partial r} + \frac{\partial}{\partial r} \left[\frac{GM(\rho + \Delta\rho)}{r} \right] \end{aligned} \quad (2)$$

Poloidal Force:

$$\begin{aligned} (\rho + \Delta\rho) \left[\frac{\partial v_\theta}{\partial t} + u_r \frac{\partial v_\theta}{\partial r} + \frac{v_\theta u_r}{r} - \cot \theta \frac{u_\phi^2}{r} - 2 \cot \theta \frac{u_\phi v_\phi}{r} + \frac{u_\phi}{r \sin \theta} \frac{\partial v_\theta}{\partial \phi} \right] = \\ - \frac{1}{r} \frac{\partial(P + \Delta P)}{\partial \theta} \end{aligned} \quad (3)$$

Azimuthal Force:

$$\begin{aligned} (\rho + \Delta\rho) \left[\frac{\partial(u_\phi + v_\phi)}{\partial t} + (u_r + v_r) \frac{\partial(u_\phi + v_\phi)}{\partial r} + \frac{v_\theta}{r} \frac{\partial u_\phi}{\partial \theta} + \cot \theta \frac{u_\phi v_\theta}{r} \right] \\ + (\rho + \Delta\rho) \left[\left(\frac{u_\phi + v_\phi}{r \sin \theta} \right) \frac{\partial(u_\phi + v_\phi)}{\partial \phi} - \frac{(u_\phi + v_\phi)(u_r + v_r)}{r} \right] = - \frac{1}{r \sin \theta} \frac{\partial(P + \Delta P)}{\partial \phi}, \end{aligned} \quad (4)$$

where ρ and $\Delta\rho$ are the initial and perturbed density respectively, u_r and v_r are the initial and perturbed radial velocities and u_ϕ and v_ϕ and the initial and perturbed azimuthal velocities. The initial poloidal velocity is zero, and its perturbed value is v_θ . P and ΔP are initial

and perturbed pressures, and GM is the gravitational constant times the enclosed mass which is dominated by that of the protoneutron star. Writing $\Delta\rho/\rho = \delta$, and assuming $\delta \propto \exp(i\omega t + \int \lambda dr) Y_{lm}(\theta, \phi)$ where $\lambda = \lambda(r)$ we derive a linearized continuity equation,

$$i\omega'\delta + v_r \left(\frac{1}{L} + \frac{2}{r} \right) + u_r \lambda \delta + \frac{imv_\phi}{r \sin \theta} + \frac{\partial v_r}{\partial r} + \frac{1}{r \sin \theta} \frac{\partial \sin \theta v_\theta}{\partial \theta} = 0, \quad (5)$$

where $\omega' = \omega + mu_\phi/r \sin \theta = \omega + m\Omega$ where $\Omega = u_\phi/r \sin \theta$ and $L = (1 - \gamma)r$ is the density scale length, defined by $\partial \ln \rho / \partial r = 1/L$. The ϕ derivatives of terms in u_ϕ and v_ϕ have been taken to yield the m dependence, but the θ derivative of the term in v_θ remains explicit. Below (in section 3.2) we will assume $u_\phi \propto r \sin \theta$ rendering Ω constant.

The radial force equation is linearized as follows. The zero order equation gives

$$\rho \frac{\partial u_r}{\partial t} + u_r \frac{\partial u_r}{\partial r} + \frac{u_\phi}{r \sin \theta} \frac{\partial u_r}{\partial \phi} = -\frac{\partial P}{\partial r} + \frac{\partial}{\partial r} \left(\frac{GM\rho}{r} \right). \quad (6)$$

If $\partial u_r / \partial \phi = 0$ and $\partial u_r / \partial t = 0$, and $\gamma = 1$ ($u_r = 0$) or $\gamma = 1.5$ ($\partial u_r / \partial r = 0$), then equation 6 evaluates to zero. We will assume that this is approximately true for all $1 \leq \gamma \leq 1.5$. (Certainly $u_r \partial u_r / \partial r < 0$ throughout this range, whereas for $\gamma > 1.5$, $u_r \partial u_r / \partial r > 0$). This helps ensure that for all cases where the postshock gas decelerates, the radial $l = 0$ mode will be stable, in agreement with the conclusions of Nakayama (1992), and Burrows & Goshy (1993) and Yamasaki & Yamada (2005), where we are assuming a neutrino luminosity below the critical value in these last two references. Taking $\Delta P = P\delta$ (i.e. an approximately isothermal perturbation; this gives a considerable simplification, see Appendix B) the equation to first order in small quantities becomes

$$\begin{aligned} & \frac{\partial}{\partial r} \left[u_r v_r \exp \int i \frac{\omega'}{u_r} dr \right] = \\ & \left[\frac{2u_\phi v_\phi}{r} - \frac{v_\theta}{r} \frac{\partial u_r}{\partial \theta} + \delta \left[\left(\frac{GM}{r} - c_s^2 \right) \lambda + \frac{2u_r^2 + u_\phi^2}{r} + \frac{u_r^2}{L} \right] \right] \exp \int i \frac{\omega'}{u_r} dr. \end{aligned} \quad (7)$$

We note that

$$\frac{d}{dr} \left[\frac{1}{i\omega'/u_r + \lambda} \exp \int \lambda + i\omega'/u_r dr \right] = \left[\frac{-d\lambda/dr + i(\omega/u_r^2) \partial u_r / \partial r}{(i\omega'/u_r + \lambda)^2} + 1 \right] \exp \int \lambda + i\omega'/u_r dr. \quad (8)$$

For a global mode we expect λ to be of order $1/r$, (in fact for $\gamma = 4/3$, $\lambda \simeq 2/r$; see equations 16 below). If ω represents laterally propagating sound waves, ω is in the range $c_s/r - c_s/|L|$, whereas $\omega \sim 2\pi(r/u_r + r/c_s)$ for radially propagating vorticity perturbations. In either case, with $\partial u_r / \partial r = (u_r/r)(3 - 2\gamma)/(\gamma - 1)$ from Appendix A, $\frac{-d\lambda/dr + i(\omega/u_r^2)(3-2\gamma)/(\gamma-1)}{(i\omega'/u_r + \lambda)^2} \ll 1$ and we may put

$$\frac{d}{dr} \left[\frac{1}{i\omega'/u_r + \lambda} \exp \int \lambda + i\omega'/u_r dr \right] \simeq \exp \int \lambda + i\omega'/u_r dr. \quad (9)$$

In equation 7 we neglect terms in u_r^2/c_s^2 , u_ϕ^2/c_s^2 (of order $(\gamma - 1)/2\gamma$) and integrate using equation 9, further assuming $|i\omega'/u_r + \lambda| \gg |1/r|$, to get

$$v_r = \frac{2u_\phi v_\phi}{i\omega' r} - \frac{v_\theta}{i\omega' r} \frac{\partial u_r}{\partial \theta} + \frac{\delta}{i\omega' + u_r \lambda} \lambda \left(\frac{GM}{r} - c_s^2 \right). \quad (10)$$

With $u_\phi = 0$ and $\partial u_r / \partial \theta = 0$, equation 7 gives

$$\frac{\partial v_r}{\partial r} u_r = \delta \left(\frac{GM}{r} - c_s^2 \right) \lambda - i\omega v_r - \frac{\partial u_r}{\partial r} v_r = \left(u_r \lambda - \frac{\partial u_r}{\partial r} \right) v_r, \quad (11)$$

where we have substituted from equation 10 for v_r to simplify the right hand side. Taking $u_r \propto r^{(3-2\gamma)/(\gamma-1)}$ from Appendix A, we derive

$$\frac{\partial v_r}{\partial r} = \left(\lambda - \frac{3 - 2\gamma}{\gamma - 1} \frac{1}{r} \right) v_r. \quad (12)$$

Expressions for v_θ and v_ϕ are easily derived in the limits $u_\phi \rightarrow 0$ or $u_r \rightarrow 0$. Staying with the nonrotating case for the time being, we give for $u_\phi = 0$:

$$\begin{aligned} v_\theta &= -\frac{c_s^2}{r} \frac{\partial \delta}{\partial \theta} \frac{1}{i\omega + \lambda u_r} \\ v_\phi &= -i \frac{m c_s^2}{r \sin \theta} \frac{\delta}{i\omega + \lambda u_r}. \end{aligned} \quad (13)$$

where the primes have been dropped from ω .

Substituting our expression for v_r , $\partial v_r / \partial r$, v_θ and v_ϕ into the linearized continuity equation (5) we find

$$i\omega \delta + \frac{\delta \lambda}{i\omega + \lambda u_r} \left(\frac{GM}{r} - c_s^2 \right) \left(\frac{1}{L} + \frac{4\gamma - 5}{\gamma - 1} \frac{1}{r} + \lambda \right) + u_r \lambda \delta + \frac{c_s^2}{i\omega + \lambda u_r} \frac{l(l+1)\delta}{r^2} = 0, \quad (14)$$

where the m dependence disappears (as it should in spherical symmetry) using properties of the spherical harmonics. This can be solved for λ to give

$$\begin{aligned} \lambda_{\pm} &= - \left(\frac{1}{2L} + \frac{4\gamma - 5}{\gamma - 1} \frac{1}{2r} \right) - \frac{i u_r \omega}{GM/r - c_s^2} \\ &\pm \left(\frac{1}{2L} + \frac{4\gamma - 5}{\gamma - 1} \frac{1}{2r} \right) \sqrt{1 + 4 \frac{i u_r \omega}{(GM/r - c_s^2)(1/L + (4\gamma - 5)/(\gamma - 1)/r)} + 4 \frac{\omega^2 - l(l+1)c_s^2/r^2}{(1/L + (4\gamma - 5)/(\gamma - 1)/r)^2 (GM/r - c_s^2)}}. \end{aligned} \quad (15)$$

We write (neglecting terms in u_r^2/c_s^2)

$$\begin{aligned} \lambda_+ \lambda_- &= \frac{l(l+1)c_s^2/r^2 - \omega^2}{GM/r - c_s^2} \\ \lambda_+ + \lambda_- &= - \left(\frac{1}{L} + \frac{4\gamma - 5}{\gamma - 1} \frac{1}{r} \right) - \frac{2i u_r \omega}{GM/r - c_s^2}. \end{aligned} \quad (16)$$

As discussed by Vishniac & Ryu (1989), a third solution exists, with $\delta = 0$ everywhere. In that case $v_r \propto \exp(-i \int \omega/u_r dr) / u_r$, and v_θ and $v_\phi \propto \exp(-i \int \omega/u_r dr) / u_r r$. The linearized continuity equation (5) then gives

$$v_r \left(\frac{1}{L} + \frac{2}{r} \right) + \frac{\partial v_r}{\partial r} + \vec{\nabla}_\perp \cdot \vec{v}_\perp = 0. \quad (17)$$

Taking $\partial v_r / \partial r = -i v_r \omega / u_r \gg v_r (1/L + 2/r)$ we find

$$v_r = \frac{u_r}{i\omega} \vec{\nabla}_\perp \cdot \vec{v}_\perp. \quad (18)$$

The derivation of the dispersion relation from the boundary conditions in terms of these three solutions is carried out in Appendix B, and given by equation B6. We use $\lambda'_\pm = \lambda_\pm / (1 + \lambda_\pm u / i\omega)$, with λ_s and λ_i evaluated at the outer shock and inner boundary respectively in terms of u_{rs} and u_{ri} , the advection velocities at these locations (see Appendix B for more details). Then in equation B6 we approximate

$$\begin{aligned} \frac{\lambda'_+ - \lambda'_- \beta^Q}{1 - \beta^Q} &= - \left(\frac{1}{2L} + \frac{4\gamma-5}{\gamma-1} \frac{1}{2r} \right) \left(1 - Q \frac{1+\beta^Q}{1-\beta^Q} \right) + \frac{i u_{ri}}{2\omega} \left(\frac{1}{2L} + \frac{4\gamma-5}{\gamma-1} \frac{1}{2r} \right)^2 \left(1 + Q \frac{1+\beta^Q}{1-\beta^Q} \right) \\ &\quad + \frac{i u_{ri} \omega}{GM/r - c_s^2} \frac{1}{Q} \frac{1+\beta^Q}{1-\beta^Q} - \frac{i u_{ri}}{\omega} \frac{l(l+1)c_s^2/r^2}{GM/r - c_s^2} \\ \frac{\lambda'_{is} - \lambda'_{+s} \beta^Q}{1 - \beta^Q} &= - \left(\frac{1}{2L} + \frac{4\gamma-5}{\gamma-1} \frac{1}{2r} \right) \left(1 + Q \frac{1+\beta^Q}{1-\beta^Q} \right) + \frac{i u_{rs}}{2\omega} \left(\frac{1}{2L} + \frac{4\gamma-5}{\gamma-1} \frac{1}{2r} \right)^2 \left(1 - Q \frac{1+\beta^Q}{1-\beta^Q} \right) \\ &\quad - \frac{i u_{rs} \omega}{GM/r - c_s^2} \frac{1}{Q} \frac{1+\beta^Q}{1-\beta^Q} - \frac{i u_{rs}}{\omega} \frac{l(l+1)c_s^2/r^2}{GM/r - c_s^2} \end{aligned} \quad (19)$$

and

$$\begin{aligned} \frac{\lambda + \lambda'_- - \lambda - \lambda'_+ \beta^Q}{1 - \beta^Q} &= \frac{l(l+1)c_s^2/r^2 - \omega^2}{GM/r - c_s^2} \left[1 - \left(\frac{1}{L} + \frac{4\gamma-5}{\gamma-1} \frac{1}{r} \right) \left(\frac{i u_{rs}}{2\omega} \left(1 + Q \frac{1+\beta^Q}{1-\beta^Q} \right) - \frac{i u_{ri}}{2\omega} \left(1 - Q \frac{1+\beta^Q}{1-\beta^Q} \right) \right) \right] \\ &\quad + \left(\frac{1}{L} + \frac{4\gamma-5}{\gamma-1} \frac{1}{r} \right) \frac{i\omega}{2(GM/r - c_s^2)} \left[u_{rs} \left(2 - Q \frac{1+\beta^Q}{1-\beta^Q} + \frac{1}{Q} \frac{1+\beta^Q}{1-\beta^Q} \right) u_{ri} \left(2 + Q \frac{1+\beta^Q}{1-\beta^Q} - \frac{1}{Q} \frac{1-\beta^Q}{1-\beta^Q} \right) \right] \end{aligned} \quad (20)$$

where we have put

$$\begin{aligned} Q' &= \sqrt{1 + 4i \frac{u_r \omega}{(GM/r - c_s^2)(1/L + (4\gamma-5)/(\gamma-1)/r)} + 4 \frac{\omega^2 - l(l+1)c_s^2/r^2}{(1/L + (4\gamma-5)/(\gamma-1)/r)^2 (GM/r - c_s^2)}} \\ &\simeq Q + \frac{2i}{Q} \frac{u\omega}{(GM/r - c_s^2)(1/L + (4\gamma-5)/(\gamma-1)/r)} \end{aligned} \quad (21)$$

and neglect terms of u^2/c_s^2 and higher. These then give

$$\begin{aligned} &\omega^4 + \omega^3 \left[i u_{rs} \left(\frac{1}{L} + \frac{5}{2r} \right) - i \frac{u_{ri}}{aL} \right] \frac{1}{Q} \frac{1+\beta^Q}{1-\beta^Q} \\ &\quad - \omega^2 \left[\frac{l(l+1)}{r^2} v_s u_r + \frac{GM/r - c_s^2}{aL} \left(\frac{1}{L} + \frac{5}{2r} \right) \right] \\ + \omega^2 &\left[\frac{GM/r - c_s^2}{2} \left(\frac{1}{L} + \frac{4\gamma-5}{\gamma-1} \frac{1}{r} \right) \left(\frac{1}{L} + \frac{5}{2r} \right) \left(1 + Q \frac{1+\beta^Q}{1-\beta^Q} \right) + \frac{GM/r - c_s^2}{2} \left(\frac{1}{L} + \frac{4\gamma-5}{\gamma-1} \frac{1}{r} \right) \frac{1}{aL} \left(1 - Q \frac{1+\beta^Q}{1-\beta^Q} \right) \right] \\ &\quad + \omega \left[i u_{rs} \left(\frac{1}{L} + \frac{5}{2r} \right) l(l+1) \frac{c_s^2}{r^2} + i \frac{u_{ri}}{aL} l(l+1) \frac{c_s^2}{r^2} + i \frac{u_{ri}}{aLQ} \frac{1+\beta^Q}{1-\beta^Q} l(l+1) \frac{v_s u_{rs}}{r^2} \right] \end{aligned}$$

$$\begin{aligned}
& +\omega \left[-\frac{i}{2} \left(\frac{GM}{r} - c_s^2 \right) \left(\frac{1}{L} + \frac{4\gamma-5}{\gamma-1} \frac{1}{r} \right)^2 \left(u_{rs} \left(\frac{1}{L} + \frac{5}{2r} \right) \left(1 - Q \frac{1+\beta^Q}{1-\beta^Q} \right) + \frac{u_{ri}}{L} \left(1 + Q \frac{1+\beta^Q}{1-\beta^Q} \right) \right) \right] \\
& \quad +\omega \left[\frac{\frac{GM}{r} - c_s^2}{2aL} \left(\frac{1}{L} + \frac{4\gamma-5}{\gamma-1} \frac{1}{r} \right) \left(\frac{1}{L} + \frac{5}{2r} \right) \left(3iu_{rs} + \frac{iu_{rs}}{Q} \frac{1+\beta^Q}{1-\beta^Q} + iu_{ri} + \frac{iu_{ri}}{Q} \frac{1+\beta^Q}{1-\beta^Q} \right) \right] \\
& \quad + \frac{GM/r - c_s^2}{aL} \left(\frac{1}{L} + \frac{5}{2r} \right) \frac{l(l+1)c_s^2}{r^2} - \frac{GM/r - c_s^2}{2aL} \left(\frac{1}{L} + \frac{4\gamma-5}{\gamma-1} \frac{1}{r} \right) \left(\frac{1}{L} + \frac{5}{2r} \right) \frac{l(l+1)v_s u_{rs}}{r^2} \left(1 - Q \frac{1+\beta^Q}{1-\beta^Q} \right) \\
& + \frac{1}{\omega} \left[\frac{GM/r - c_s^2}{2al} \left(\frac{1}{L} + \frac{5}{2r} \right) l(l+1) \frac{c_s^2}{r^2} \left(\frac{1}{L} + \frac{4\gamma-5}{\gamma-1} \frac{1}{r} \right) \left(-iu_{rs} \left(1 + Q \frac{1+\beta^Q}{1-\beta^Q} \right) - iu_{ri} \left(1 - Q \frac{1+\beta^Q}{1-\beta^Q} \right) \right) \right] \\
& \quad \frac{1}{\omega} \left[-\frac{l(l+1)v_s u_{rs}}{r^2} \left(i \frac{u_{ri}}{2aL} (GM/r - c_s^2) \left(\frac{1}{L} + \frac{4\gamma-5}{\gamma-1} \frac{1}{r} \right)^2 \left(1 + Q \frac{1+\beta^Q}{1-\beta^Q} \right) + i \frac{u_{ri}}{aL} \frac{l(l+1)c_s^2}{r^2} \right) \right] = 0 \quad (22)
\end{aligned}$$

If $u_r = 0$, equation 22 is very similar to equation 13a of Vishniac & Ryu (1989), and is identical if we take $r \rightarrow \infty$, $L \rightarrow -L$ (to agree with their sign convention), $l(l+1)/r^2 \rightarrow k^2$ and $\gamma \rightarrow 1$ (i.e. $v_s u_r \rightarrow c_s^2$). In their case the limit $Q \rightarrow 1$ gives a dispersion relation similar to the exact solution in the thin shock limit (Vishniac 1983), and identical to this limit if terms describing the evolution of the shock are neglected from the exact solution. They then proceed to argue that taking $Q \neq 1$ gives a suitable approximate dispersion relation away from the thin shock limit. Our case is particularly suitable since the standing accretion shock can be treated as an equilibrium state (Burrows & Goshy 1993), i.e. it does not evolve in our approximation.

Just taking $u_r = 0$, equation 20 yields a quadratic equation in ω^2 for which simple solutions exist. Vishniac & Ryu (1989) find growing shock oscillations in the case of decelerating shocks, with a post shock rarefaction. In our case, the growing oscillations exist for density increasing with distance behind the shock. This difference arises because the square of the sound speed, $c_s^2 \rightarrow c_s^2 - GM/r$ in our case, and $GM/r > c_s^2$. When $u_r = 0$ (except in terms in $v_s u_r$) and taking $Q \rightarrow 1$,

$$\begin{aligned}
\omega^2 &= \frac{l(l+1)v_s u_r}{2r^2} - \left(\frac{GM}{r} - c_s^2 \right) \left(\frac{1}{2L} + \frac{5}{4r} \right) \frac{4\gamma-5}{\gamma-1} \frac{1}{r} \\
&\pm \left\{ \frac{l(l+1)v_s u_r}{2r^2} - \left(\frac{GM}{r} - c_s^2 \right) \left(\frac{1}{2L} + \frac{5}{4r} \right) \frac{4\gamma-5}{\gamma-1} \frac{1}{r} \right\} \sqrt{1-W}. \quad (23)
\end{aligned}$$

where

$$W = 4 \frac{\left(\frac{GM}{r} - c_s^2 \right) \frac{1}{L} \left(\frac{1}{L} + \frac{5}{2r} \right) \frac{l(l+1)v_s u_r}{r^2}}{\left\{ \frac{l(l+1)v_s u_r}{r^2} - \left(\frac{GM}{r} - c_s^2 \right) \left(\frac{1}{L} + \frac{5}{2r} \right) \frac{4\gamma-5}{\gamma-1} \frac{1}{r} \right\}^2} \quad (24)$$

When $1 \gg W$, this gives a pair of sound waves for given l with

$$\omega^2 \simeq l(l+1) v_s u_r / r^2 - (GM/r^2 - c_s^2/r) (1/L + 5/2r) \frac{4\gamma-5}{\gamma-1} \quad (25)$$

taking the positive sign, and the negative sign gives a pair of gravity waves with

$$\omega^2 \simeq 2 \frac{\left(\frac{GM}{r} - c_s^2 \right) \frac{1}{L} \left(\frac{1}{L} + \frac{5}{2r} \right) \frac{l(l+1)v_s u_r}{r^2}}{\left\{ \frac{l(l+1)v_s u_r}{r^2} - \left(\frac{GM}{r} - c_s^2 \right) \left(\frac{1}{L} + \frac{5}{2r} \right) \frac{4\gamma-5}{\gamma-1} \frac{1}{r} \right\}}, \quad (26)$$

where a is a constant coming into our definition of the interior boundary condition, as explained in Appendix B. For $1 < W$, we have four roots of the form $\omega = \pm(f + ig)$ and $\omega = \pm(f - ig)$, and all roots have a combined character of acoustic and gravity waves. Reinstating the terms in odd powers of ω with nonzero u_r , the roots separate into pairs of what may be termed acoustic and gravity waves, although the difference in frequency between them is generally rather small and both pairs are of presumably mixed character, and one imaginary (i.e. purely growing or damping) mode. Assuming a value of Q , we solve the quintic equation numerically. Results for each growing mode are then iterated until the value of Q produced by the frequency and wavenumber matches the input. Results of this procedure for growing modes are given in Table 1 for $\gamma = 4/3$, $a = 1.5$, and in Table 2 for $\gamma = 1.36$, $a = 2$, the values of a being chosen to reproduce as far as possible the stability properties of the radial mode. We compare in each case the results of the full quintic equation with a simpler case taking $u_{rs} = u_{ri} = 0$.

With $\gamma = 4/3$, taking $GM/rc_s^2 \simeq 1/(\gamma - 1) = 3$ (from equation A2 neglecting u_r^2), and without advection, we find growth for $l = 1$ for all values of $r_s/r_i \leq 0.1$. Growth at $l = 1$ at $r_s/r_i \rightarrow \infty$ and at $l = 2$ for all r_s/r_i require non-zero advection terms in the dispersion relation, though the $l = 2$ mode is stable as $r_s/r_i \rightarrow \infty$, even in the presence of advection. The $l = 0$ mode is marginally stable in the absence of advection. With advection included, it is stable for the lowest r_s/r_i , but otherwise unstable. Taken together, there is reasonable qualitative agreement with Blondin & Mezzacappa (2006), but quantitatively, the model is less stable than it should be. Growth rates are too high, and the $l = 0$ mode becomes unstable too quickly as r_s/r_i increases. Better qualitative and quantitative agreement is found in the model with $\gamma = 1.36$ and $a = 2$ given in Table 2., and also illustrated in Figure 2. The stability of $l = 0$ is improved, and advection becomes relatively more necessary to the instability of $l = 1$. These results have a simple interpretation in terms of the mechanisms put forward by Blondin & Mezzacappa (2006) and Foglizzo et al. (2007). Where advection is not necessary to the instability, i.e. for the $l = 1$ mode at low values of r_s/r_i , the wave growth must be due to trapped sound waves similarly to the simulations of Blondin & Mezzacappa (2006). The inclusion of advection in these cases generally increases the growth rate, either due to a separate contribution of an “advective-acoustic” nature or because of the effect of postshock advection on the propagation of sound waves. In cases where no instability occurs unless advection terms are present, the growth must be due to an advective-acoustic cycle similar to Foglizzo et al. (2007). In our model, these cases include all the $l = 2$ modes, as well as the $l = 1$ modes for large values of r_s/r_i .

These results and interpretation add a new twist to the conclusions of Foglizzo et al. (2007). These authors demonstrate that for $r_s/r_i > 10$ the advective-acoustic cycle is the cause of the $l = 1$ instability. Their analysis makes use of a WKB approximation that

is not valid for lower r_s/r_i . However they proceed to argue that since growth rates and frequencies vary smoothly as one goes to lower values of r_s/r_i , the mechanism of instability should remain the same. However our results suggests that even though the eigenvalues vary smoothly, the mechanism of instability changes to more closely resemble that suggested by Blondin & Mezzacappa (2006).

3. Discussion

3.1. Preamble

A number of simplifying assumptions have been introduced into the analysis to make the algebra tractable. We have assumed an isothermal perturbation, used a greatly simplified interior boundary condition, and have dropped all terms in the advection velocity of order higher than u_r/c_s . Nevertheless our model appears to capture the basic features of the numerical simulations of Blondin & Mezzacappa (2006), *and* the analytic theory of Foglizzo et al. (2007) and Galletti & Foglizzo (2005), in the appropriate regions of parameter space. Looking at the values of λ_{\pm} given by equation 15, we find when $\omega^2 \sim l(l+1)c_s^2/r^2$, $|\lambda_-| \gg |\lambda_+|$, $\lambda_- > 0$ and $\lambda_+ \gtrsim 0$ for $Q \lesssim 1$. Consequently, λ_- gives a density perturbation $\delta = \delta\rho/\rho$ that is greatest at the outer shock and considerably smaller at the inner boundary, while λ_+ gives a density perturbation that varies much less with radius, but can be largest at the outer shock or at the inner boundary. When $l = 0$, $\lambda_+ < 0$ and $|\lambda_-| \sim |\lambda_+|$. In this case the radial mode can have a large maximum of δ at the inner boundary. Given the ad hoc nature of our inner boundary condition (see Appendix B), we might expect less accurate results for the radial mode than for nonradial modes, which does indeed seem to be the case. The vorticity (calculated from equations 13) increases inwards approximately as δ/r^2 . The third solution with $\delta = 0$ everywhere must represent a purely vortical perturbation.

3.2. The Mechanism of Instability

So far we have developed a dispersion relation from the equations of hydrodynamics, and found instabilities through the existence of complex roots. We have not made any comment on the precise mechanism of the instability, other than to comment that sound/gravity waves appear to grow. The vortical-acoustic cycle has been explained by Foglizzo (2002). A distortion of the accretion shock produces a vorticity perturbation that is advected inwards. Upon reaching the inner boundary, the vorticity perturbation produces an upward moving sound wave, which reinforces the shock distortion when it arrives there, producing a net

increase in the original perturbation. Over many cycles, exponential growth ensues.

Sound waves produced at the outer shock, in a realistic model, will not propagate towards the center due to the effects of refraction. Instead, they will propagate around the circumference of the shock. Blondin & Mezzacappa (2006) speculate that sound waves produced at one position on the shock surface by a density inhomogeneity will propagate around until they meet on the opposite side, where their excess pressure produces a shock distortion that sends another pair of sound waves back again. It is not immediately clear without detailed calculation that such a process should produce a growing (as opposed to damping) oscillation. We speculate that growth must also be aided by the flow of plasma in through the accretion shock. In Figure 3 we show flowlines for shocked plasma in an accretion shock with a 10% $l = 1$ modulation of the shock radius. When the shock is shifted up by the instability, incoming plasma in the equatorial regions is diverted downwards by the now oblique shock. This non-radial flow of shocked plasma enhances the oscillation and leads to further wave growth. This aspect is similar to the thin shell overstability of decelerating shocks (Vishniac 1983; Vishniac & Ryu 1989), (although Velikovich et al. (2005) put forward a different view), though in these cases the pressure produced by gravitational confinement plays no role, and overstability exists for a postshock density gradient oppositely directed to our case. Thus both the advective-acoustic (or vortical-acoustic) instability and the growth due to trapped sound waves have their origins in perturbations of either vorticity or pressure in the post shock flow produced by the distorted shock front.

3.3. The Effect of Rotation

There is considerable interest in the effects of rotation on core-collapse explosions. In particular, in which direction with respect to the rotation axis should one expect the strongest growth? This would have obvious implications for the directions of pulsar kicks, assuming the such instabilities are the correct mechanism. In the case of an advective-acoustic instability, we should expect the decrease in the postshock advection in the plane of rotation to give stronger instability and hence strongest growth along the axis of rotation.

In the case of instability driven by trapped sound waves we can sketch out the effect of including a nonzero u_ϕ in the forgoing analysis. We derive the extra terms to be included in the dispersion relation in the limits $u_r \rightarrow 0$ and $u_\phi^2/c_s^2 \rightarrow 0$. We also neglect any distortion of the shock front by the rotation. Such considerations require more detailed physics, neutrino cooling near the inner boundary at a minimum (Blondin & Mezzacappa 2006), and ideally also neutrino luminosities and mass accretion rates (see e.g. Burrows & Goshy 1993; Yamasaki & Yamada 2005), and are beyond the scope of this paper. This keeps $u_\theta = 0$,

which should be true in any case if $u_r = 0$, but even in the absence of advection, a distortion of the shock front may change the boundary condition leading to equation B2. The perturbed velocities are

$$\begin{aligned} v_r &= \frac{\delta\lambda}{i\omega'} \left(\frac{GM}{r} - c_s^2 \right) - \frac{2m\Omega c_s^2 \delta}{ir\omega'^2} \\ v_\theta &= -\frac{2mc_s^2 \Omega \delta \cot \theta}{ir\omega'^2} - \frac{c_s^2}{ir\omega'} \frac{\partial \delta}{\partial \theta} \\ v_\phi &= -\frac{mc_s^2 \delta}{\omega' r \sin \theta} + \frac{2\Omega \delta \lambda \sin \theta}{\omega'^2} \left(\frac{GM}{r} - c_s^2 \right) - \frac{2\Omega c_s^2 \cos \theta}{r\omega'^2} \frac{\partial \delta}{\partial \theta}. \end{aligned} \quad (27)$$

With

$$\frac{\partial v_r}{\partial r} = -\frac{v_r}{r} + \frac{\delta (GM/r - c_s^2) \lambda^2}{i\omega'}, \quad (28)$$

the linearized continuity equation becomes

$$-\omega'^2 + \left\{ \left(\frac{GM}{r} - c_s^2 \right) \lambda - \frac{2m\Omega c_s^2}{r\omega'} \right\} \left(\frac{1}{L} + \frac{1}{r} \right) + \lambda^2 \left(\frac{GM}{r} - c_s^2 \right) + \frac{l(l+1)c_s^2}{r^2} + \frac{2mc_s^2 \Omega}{r^2 \omega'} - \frac{2mc_s^2 \Omega \lambda}{r\omega'} = 0 \quad (29)$$

after dividing through by δ , with solutions for λ_\pm

$$\begin{aligned} \lambda_+ + \lambda_- &= -\left(\frac{1}{L} + \frac{1}{r} \right) + \frac{2\Omega m}{r\omega'} \\ \lambda_+ \lambda_- &= \frac{l(l+1)c_s^2/r^2 - \omega'^2}{GM/r - c_s^2} - \frac{2m\Omega c_s^2}{rL\omega'} \frac{1}{GM/r - c_s^2}. \end{aligned} \quad (30)$$

We again have $v_r \propto \exp \int -i\omega'/u_r dr$ if $\delta = 0$, so equation (14) still holds. Then, with unchanged boundary conditions, the dispersion relation is the same as before (with $u_r = 0$ and $\omega \rightarrow \omega'$ in equation B6), but with the extra terms (neglecting the change $1/L + (4\gamma - 5)/(\gamma - 1)/r \rightarrow 1/L + 1/r$, which in any case is trivial for $\gamma = 4/3$)

$$\begin{aligned} &\omega' \frac{m\Omega}{r} \left(\frac{GM}{r} - c_s^2 \right) \left(\frac{2}{L} + \frac{5}{2r} Q \frac{1+\beta Q}{1-\beta Q} \right) \\ &- \frac{l(l+1)v_s u_r}{r^2} \frac{m\Omega}{\omega' r} \left(\frac{GM}{rL} - \frac{c_s^2}{L} \right) \left(1 - Q \frac{1+\beta Q}{1-\beta Q} \right) - \left(\frac{GM}{rL} - \frac{c_s^2}{L} \right) \left(\frac{1}{L} + \frac{5}{2r} \right) \frac{2m\Omega c_s^2}{rL\omega'}. \end{aligned} \quad (31)$$

The new quintic equation is again solved numerically, with results given in Table 3 for the $m = 1$ component of the $l = 1$ mode. We generally find higher growth rates increasing with rotation rate for the $m = 1$ ($m = 0$ remains unchanged), which would indicate higher growth in the plane of rotation. This happens even in cases where in the absence of rotation, the advective-acoustic instability seems to be dominant. We speculate that rotation increases the growth rate of trapped sound waves for nonzero m , so much so that they can grow even in cases with zero growth in the absence of rotation.

At higher rotation rates, the distortion of the shock front cannot be neglected. We expect the equilibrium shock position to be oblate, i.e. bulging out at the equator as demonstrated quantitatively by Yamasaki & Yamada (2005). We emphasize again that our results are not applicable in this regime.

4. Conclusions

Using heuristic arguments based on Vishniac & Ryu (1989), and a few other approximations, we have derived an approximate dispersion relations for oscillations of a standing spherical accretion shock. The pursuit of an analytic treatment further through the problem than has previously been attempted arguably allows greater physical insight, albeit at the expense of reduced quantitative accuracy. While our model might not be considered much more than a “toy model”, it does capture most of the features of previous works of the instability of such shocks. It offers a potential resolution to the mild disagreement between the works of Blondin & Mezzacappa (2006) and Foglizzo et al. (2007). We find results consistent with both works, but in different regions of parameter space. For low values of r_s/r_i , the growth of trapped waves dominates in the $l = 1$, and appears to be the most important mechanism. The inclusion of post shock advection gives a small change, usually an increase, in the growth rate. At higher l , or r_s/r_i , postshock advection appears to become crucial to the instability, which leads us to interpret it as an advective-acoustic cycle. In a treatment of $\gamma = 4/3$ gas in core collapse supernovae, Galletti & Foglizzo (2005) only find advective-acoustic instability for $r_s/r_i > 3.5$, with the growth rate increasing out to $r_s/r_i \sim 10$. Foglizzo et al. (2007) are only able to demonstrate the operation of the advective-acoustic cycle for $r_s/r_i \geq 10$, due to the nature of the approximations involved, but conjecture that it should also operate at lower r_s/r_i . Our models agree with their demonstrations at large shock radii, but suggest that at smaller shock radius, the instability should change to resemble that observed by Blondin & Mezzacappa (2006).

The precise mechanism of instability probably becomes more significant in the rotating case. The advective-acoustic instability must grow preferentially along the rotation axis, where the postshock advection is not affected by the rotation. By contrast, we conjecture in section 3.3 that rotation should enhance the growth of trapped sound/gravity waves principally in the plane of rotation, leading to stronger growth in directions perpendicular to the rotation axis. Such effects may have important consequences for pulsar natal kicks, if these derive from hydrodynamic kick mechanisms.

This work has been supported by the Chandra GI Program, the NASA LTSA and APRA programs, and by basic research funds of the Office of Naval Research. I acknowledge a scientific discussion with Ethan Vishniac, and an extremely careful and constructive reading of the paper by an anonymous referee.

A. Bernoulli Equation for the Postshock Flow

Here we summarize the model for the postshock flow in spherical accretion used by Blondin, Mezzacappa & DeMarino (2003). The flow is given by the Bernoulli equation

$$u_r^2 + \frac{2\gamma}{\gamma-1} \frac{P}{\rho} - \frac{2GM}{r} = 0 \quad (\text{A1})$$

and just behind the shock itself the jump conditions give the velocity, density and pressure as

$$\begin{aligned} u_r &= -\frac{\gamma-1}{\gamma+1} \sqrt{\frac{2GM}{r_s}} \\ \rho &= \frac{\gamma+1}{\gamma-1} \frac{\dot{M}}{4\pi} \sqrt{\frac{r_s}{2GM}} \frac{1}{r_s^2} \\ P &= \frac{2}{\gamma+1} \frac{\dot{M}}{4\pi} \sqrt{\frac{2GM}{r_s}} \frac{1}{r_s^2}. \end{aligned} \quad (\text{A2})$$

Evaluating $P/\rho^\gamma = \text{constant}$ from the jump conditions and substituting gives

$$r' u_r'^2 + \frac{4\gamma}{(\gamma+1)(\gamma-1)} \left(\frac{\gamma-1}{\gamma+1} \right)^\gamma r'^{3-2\gamma} u_r'^{1-\gamma} - 1 = 0 \quad (\text{A3})$$

where $r' = r/r_s$ and $u' = u_r \sqrt{r_s/2GM}$. Neglecting the first term (i.e the kinetic energy), $u_r \propto r^{(3-2\gamma)/(\gamma-1)}$ and hence $\rho \propto r^{-1/(\gamma-1)}$. These results are exact for $\gamma = 5/3$. In this approximation, the density decreases monotonically with increasing radial distance, and L defined above is $L = r(1-\gamma)$. We note that for $\gamma \rightarrow 1$, close to the shock, the density may increase with increasing radial distance, i.e. a postshock rarefaction exists. For $\gamma = 1$, this region extends between $0.75r_s < r < r_s$, and disappears for $\gamma > 1.1$.

B. Boundary Conditions and Dispersion Relation

We recapitulate and modify very slightly the approach of Vishniac & Ryu (1989). Let B_\pm be the amplitudes of the λ_\pm oscillations of the accretion shock. Then at the accretion shock, $\delta(0) = -\delta r_s/L - 5\delta r_s/2r_s - 2\delta v_s/v_s \simeq -\delta r_s/L - 5\delta r_s/2r_s = -(1/L + 5/2r) v_r/i\omega$, which comes from the radial variation of the shock ram pressure. We follow Vishniac & Ryu (1989) and neglect the term in δv_s , which renders the perturbation isothermal. Blondin & Mezzacappa (2006) also comment that the term in δv_s is smaller by a factor of a few than the term in δr_s in determining the shock ram pressure. Hence

$$B_+ + B_- = \left(\frac{(GM/r - c_s^2)}{\omega^2} (B_+ \lambda'_{+s} + B_- \lambda'_{-s}) + \frac{u_r \nabla_\perp \cdot v_\perp}{\omega^2} \right) \left(\frac{1}{L} + \frac{5}{2r} \right), \quad (\text{B1})$$

where $\lambda'_\pm = \lambda_\pm / (1 + \lambda_\pm u / i\omega)$, and the subscript s indicates that this is evaluated at the outer shock.

Also at the accretion shock, $v_\perp(r_s) = v_s \vec{\nabla}_\perp \delta r_s = (v_s / i\omega) \vec{\nabla}_\perp v_r(r_s)$, which after some rearrangement gives

$$\vec{\nabla}_\perp \cdot \vec{v}_\perp = -\frac{v_s (GM/r - c_s^2)}{\omega^2} \nabla_\perp^2 (B_+ \lambda'_{+s} + B_- \lambda'_{-s}) - \frac{v_s u_r}{\omega^2} \nabla_\perp^2 (\vec{\nabla}_\perp \cdot \vec{v}_\perp). \quad (\text{B2})$$

Eliminating $\vec{\nabla}_\perp \cdot \vec{v}_\perp$ between equations B1 and B2 gives

$$\begin{aligned} & B_+ \left(\omega^2 L' \left(1 - \frac{v_s u_r l(l+1)}{\omega^2 r^2} \right) - \left(\frac{GM}{r} - c_s^2 \right) \lambda'_{+s} \right) + \\ & B_- \left(\omega^2 L' \left(1 - \frac{v_s u_r l(l+1)}{\omega^2 r^2} \right) - \left(\frac{GM}{r} - c_s^2 \right) \lambda'_{-s} \right) = 0 \end{aligned} \quad (\text{B3})$$

where $\nabla_\perp^2 B_\pm = -l(l+1) B_\pm / r^2$, $\nabla_\perp^2 (\vec{\nabla}_\perp \cdot \vec{v}_\perp) = -l(l+1) (\vec{\nabla}_\perp \cdot \vec{v}_\perp) / r^2$ and $1/L' = 1/L + 5/2r$.

The interior boundary, and hence the boundary conditions here, are less well defined in our model. We are assuming that the region where strong neutrino cooling sets in and causes the accreting matter to decouple from the hot postshock flow will give a boundary from which waves can reflect. Vishniac & Ryu (1989), considering a plane parallel shock, assume a constant pressure boundary condition, $\delta = -\delta r_i / L = -v_r / i\omega L$. We assume something similar;

$$\delta(r_i) = B_+ \exp \int_{r_i}^{r_s} \lambda_+ dr + B_- \exp \int_{r_i}^{r_s} \lambda_- dr = -\frac{v_r(r_i)}{i\omega a L} = -\frac{\delta(r_i) (GM/r - c_s^2)}{\omega^2 a L}. \quad (\text{B4})$$

We do not take the local value of L in this boundary condition, but take the same value as assumed above at the forward shock, modified by a constant a which we vary to find the best match to the $l = 0$ stability. In any case, $\delta(r_i) = -v_r(r_i) / i\omega a L(r_s) \ll -v_r(r_i) / i\omega L(r_i)$ as it must be, because the background density increases significantly over that predicted by the Bernoulli model due to radiative cooling by neutrino emission. We prefer to cast the interior boundary condition in terms of L and r evaluated at the outer shock, because of the algebraic simplification it produces, and the somewhat easier conditions required to keep the $l = 0$ mode stable. It is clear from the work of various authors Nakayama (e.g. 1992); Burrows & Goshy (e.g. 1993); Yamasaki & Yamada (e.g. 2005) that this must be true. These last two references, in particular, include considerably more physics, and are able to predict the shock radius, rather than just specifying it as we do, but they only treat radial stability. Consequently we have

$$B_+ \exp \int_{r_i}^{r_s} (\lambda_+ - \lambda_-) dr \left\{ 1 - \frac{1}{\omega^2 a L} \left[\left(\frac{GM}{r} - c_s^2 \right) \lambda'_{+i} \right] \right\} + B_- \left\{ 1 - \frac{1}{\omega^2 a L} \left[\left(\frac{GM}{r} - c_s^2 \right) \lambda'_{-i} \right] \right\} = 0, \quad (\text{B5})$$

where the $\lambda_{\pm i}$ are evaluated with u at the inner boundary, but otherwise with L and r at the outer shock.

Now eliminating B_+/B_- between equations B3 and B5 gives the dispersion relation:

$$\begin{aligned} & \omega^4 [1 - \beta^Q] - \omega^2 \frac{l(l+1)}{r^2} v_s u_r [1 - \beta^Q] - \omega^2 \left(\frac{GM}{r} - c_s^2 \right) \frac{1}{aL} [\lambda'_{+i} - \lambda'_{-i} \beta^Q] \\ & - \omega^2 \left(\frac{GM}{r} - c_s^2 \right) \left(\frac{1}{L} + \frac{5}{2r} \right) [\lambda'_{-s} - \lambda'_{+s} \beta^Q] + \frac{l(l+1)}{r^2} v_s u_r \left(\frac{GM}{r} - c_s^2 \right) \frac{1}{aL} [\lambda'_{+i} - \lambda'_{-i} \beta^Q] \\ & + \left(\frac{GM}{r} - c_s^2 \right)^2 \frac{1}{aL} \left(\frac{1}{L} + \frac{5}{2r} \right) [\lambda'_{+i} \lambda'_{-s} - \lambda'_{+s} \lambda'_{-i} \beta^Q] = 0 \end{aligned} \quad (\text{B6})$$

where

$$\beta^Q = \exp \int_{r_i}^{r_s} -(\lambda_+ - \lambda_-) dr = \exp \int_{r_i}^{r_s} \left(\frac{1}{L} + \frac{4\gamma - 5}{\gamma - 1} \frac{1}{r} \right) Q dr \simeq \left(\frac{r_i}{r_s} \right)^{\frac{6-4\gamma}{\gamma-1} Q}. \quad (\text{B7})$$

For $1 < \gamma < 1.5$, $\beta \rightarrow 0$ as $r_i/r_s \rightarrow 0$, and as $\gamma \rightarrow 1$ for fixed r_s/r_i .

REFERENCES

- Blondin, J. M., Mezzacappa, A., & DeMarino, C. 2003, ApJ, 584, 971
- Blondin, J. M., & Mezzacappa, A. 2006, ApJ, 642, 401
- Burrows, A., Livne, E., Dessart, L., Ott, C. D., & Murphy, J. 2006, ApJ, 640, 878
- Burrows, A., & Goshy, J. 1993, ApJ, 416, L75
- Chandrasekhar, S. 1961, Hydrodynamic and Hydromagnetic Stability (New York: Dover)
- Foglizzo, T. 2002, A&A, 392, 353
- Foglizzo, T., Scheck, L., & Janka, H.-Th. 2006, ApJ, 652, 1436
- Foglizzo, T., Galletti, P., Scheck, L., & Janka, H.-Th. 2007, ApJ, 654, 1006
- Galletti, P., & Foglizzo, T. 2005, in proceedings of the SF2A meeting, 17-30 June 2005, Strasbourg, EDPS Conference Series in Astronomy and Astrophysics, ed. F. Casoli, T. Contini, H. M. Hameury & L. Pagani, astro-ph/0509635
- Herant, M., Benz, W., & Colgate, S. 1992, ApJ, 395, 642
- Herant, M. 1995, Physics Reports, 256, 117

Janka, H.-Th. 2001, *A&A*, 368, 527

Kifonidis, K., Plewa, T., Scheck, L., Janka, H.-Th., & Müller, E. 2005, *A&A*, 453, 661

Nakayama, K. 1992, *MNRAS*, 259, 259

Ohnishi, N., Kotake, K., & Yamada S. 2006, *ApJ*, 641, 1018

Scheck, L., Plewa, T., Janka, H.-Th., Kifonidis, K., & Müller, E. 2004, *Phys. Rev. Lett.*, 92, 011103-1

Scheck, L., Kifonidis, K., Janka, H.-Th., & Müller, E. 2006, *A&A*, 457, 963

Velikovich, A. L., Zalesak, S. T., Metzler, N. & Wouchuk, J. G. 2005, *Phys. Rev. E*, 72, 046306

Vishniac, E. T., & Ryu, D. 1989, *ApJ*, 339, 917

Vishniac, E. T. 1983, *ApJ*, 274, 152

Yamasaki, T., & Yamada, S. 2005, *ApJ*, 623, 1000

Yamasaki, T., & Yamada, S. 2006, *ApJ*, submitted, astro-ph/0606581

Table 1: Eigenvalues of growing modes $0 \leq l \leq 2$: $\gamma = 4/3$, $a = 1.5$

r_s/r_i	no advection			advection		
	$l = 0$	$l = 1$	$l = 2$	$l = 0$	$l = 1$	$l = 2$
2	± 0.569	± 0.525 $-0.242i$		± 0.569 $+0.034i$	± 0.546 $-0.284i$	± 0.771 $-0.326i$
3	± 0.391	± 0.443 $-0.253i$		± 0.447 $-0.090i$	± 0.520 $-0.305i$	± 0.730 $-0.312i$
5	± 0.257	± 0.387 $-0.248i$		± 0.453 $-0.155i$	± 0.511 $-0.310i$	± 0.707 $-0.297i$
10	± 0.145	± 0.342 $-0.238i$		± 0.479 $-0.178i$	± 0.516 $-0.311i$	± 0.693 $-0.287i$
∞				± 0.511 $-0.199i$	± 0.532 $-0.311i$	

Note. — Real and imaginary frequencies are in units of $|c_s/L|$. Growing modes have a negative imaginary part.

Table 2: Eigenvalues of growing modes $0 \leq l \leq 2$: $\gamma = 1.36$, $a = 2$

r_s/r_i	no advection			advection		
	$l = 0$	$l = 1$	$l = 2$	$l = 0$	$l = 1$	$l = 2$
2	± 0.506	± 0.495 $-0.193i$		± 0.523 $+0.010i$	± 0.490 $-0.222i$	± 0.829 $-0.173i$
3	± 0.347	± 0.404 $-0.175i$		± 0.353 $+0.500i$	± 0.454 $-0.228i$	± 0.818 $-0.171i$
5	± 0.219			± 0.264 $-0.058i$	± 0.425 $-0.220i$	± 0.811 $-0.176i$
10	± 0.044			± 0.287 $-0.11i$	± 0.401 $-0.201i$	± 0.806 $-0.194i$
∞				± 0.343 $-0.147i$	± 0.383 $-0.119i$	

Note. — Real and imaginary frequencies are in units of $|c_s/L|$. Growing modes have a negative imaginary part.

Table 3: Eigenvalues of $l = 1, m = 1, \gamma = 1.36, a = 2$

r_s/r_i	u_ϕ					
	0.0	0.05	0.1	0.2	0.3	0.4
2	-0.490	-0.498	-0.502	-0.511	-0.520	-0.527
	$-0.222i$	$-0.231i$	$-0.242i$	$-0.264i$	$-0.282i$	$-0.298i$
	0.490	0.489	0.484	0.473	0.461	
	$-0.222i$	$-0.205i$	$-0.190i$	$-0.154i$	$-0.091i$	
10	0.401	0.430	0.433	0.441	0.449	0.456
	$-0.201i$	$-0.224i$	$-0.241i$	$-0.264i$	$-0.281i$	$-0.294i$
	-0.401	-0.425	-0.430	-0.464	-0.483	-0.495
	$-0.201i$	$-0.171i$	$-0.115i$	$-0.045i$	$-0.032i$	$-0.027i$

Note. — Real ($\omega' = \omega + m\Omega$) and imaginary frequencies are in units of $|c_s/L|$. Growing modes have a negative imaginary part. For $m = -1$, real parts take opposite signs.

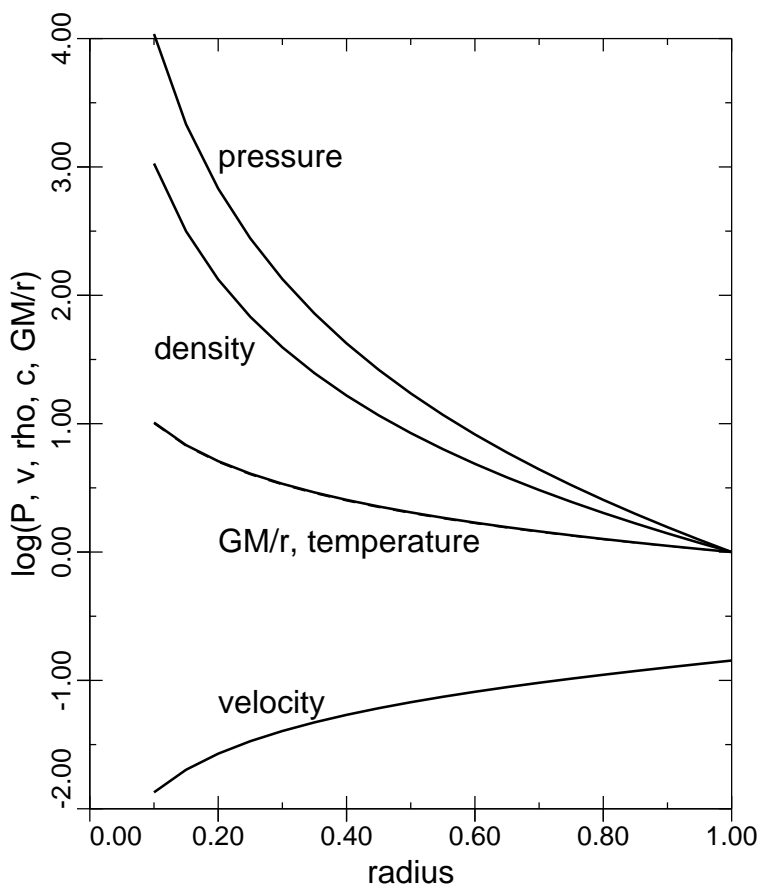


Fig. 1.— Variation behind the accretion shock of the pressure, density, inward flow velocity, sound speed and gravitational potential for a $\gamma = 4/3$ model. All quantities are normalized to unity at the accretion shock and radius unity, except the inward flow velocity, which is $1/7$, the shock velocity being unity at radius =1. The pressure and density exhibit much bigger variations with distance than any other quantity, motivating us to simplify the problem by taking the sound speed, inward flow velocity and gravitational potential to be constant throughout the shocked plasma.

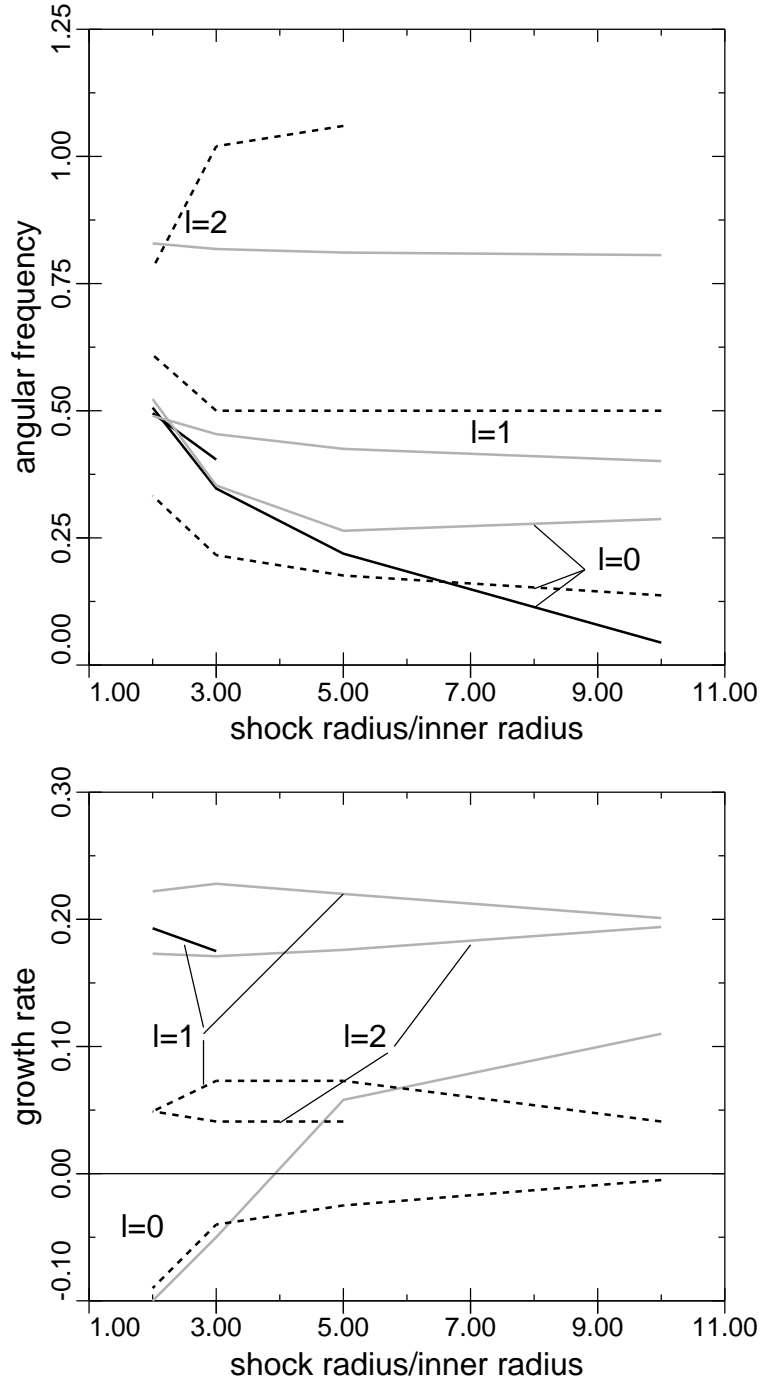


Fig. 2.— Angular frequencies and growth rates of unstable modes plotted against r_s/r_i . Solid lines give present results, (black without advection; grey with advection), and the dashed lines are those from Blondin & Mezzacappa (2006), all in units of c_s/L evaluated close to the accretion shock. The growth rate of the $l = 0$ mode without advection is 0; it is only marginally stable, and is not plotted.

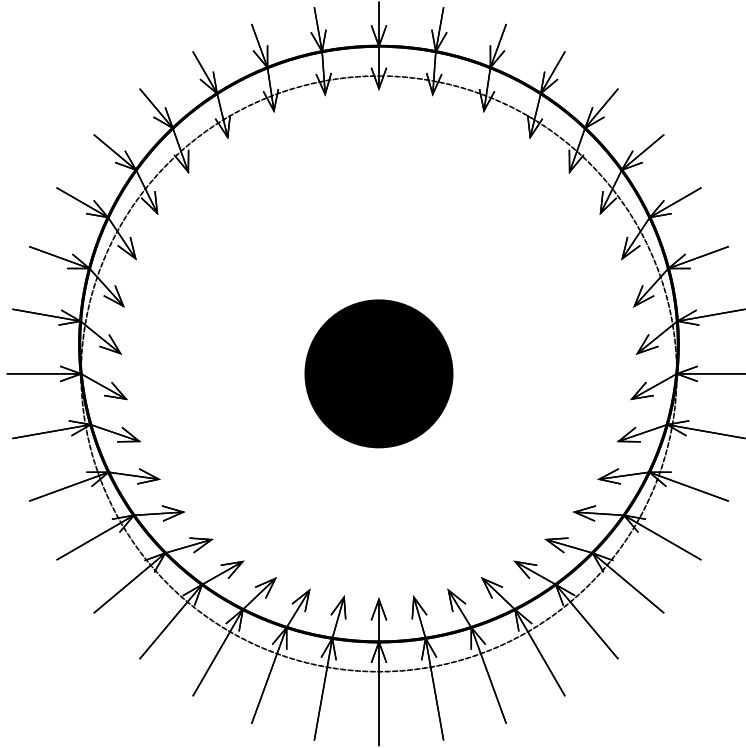


Fig. 3.— Post shock advection velocity flow lines for an accretion shock with 10% $l = 1$ modulation of radius for $\gamma = 4/3$ (upper panel). The shock perturbed upwards (solid line) from its equilibrium position (dashed line) has its surface distorted such that incoming plasma flows preferentially towards the lower density and pressure region at the bottom of the figure. This helps induce the growing oscillation.